arXiv:1203.0623v3 [cond-mat.quant-gas] 28 Oct 2012

Interatomic collisions in two-dimensional and quasi-two-dimensional confinements with spin-orbit coupling

Peng Zhang,[1] Long Zhang,[2] and Wei Zhang*[1]
[1]Department of Physics, Renmin University of China, Beijing, 100190, China
[2]Hefei National Laboratory for Physical sciences at Microscale,
University of Science and Technology of China, Hefei, Anhui 230027, China

We investigate the low-energy scattering and bound states of two two-component fermionic atoms in pure two-dimensional (2D) and quasi-2D confinements with Rashba spin-orbit coupling (SOC). We find that the SOC qualitatively changes the behavior of the 2D scattering amplitude in the low-energy limit. For quasi-2D systems we obtain the analytic expression for the effective-2D scattering amplitude and the algebraic equations for the two-atom bound state energy. We further derive the effective 2D contact potential for the interaction between ultracold atoms in the quasi-2D confinement. This effective potential can be used in the research on many-body physics of quasi-2D ultracold fermi gases with Rashba SOC.

PACS numbers: 34.50.-s, 03.65.Nk

I. INTRODUCTION

The discussion on synthetic gauge field [1] and spin-orbit coupling (SOC) [2] in bosonic and fermionic systems has recently drawn great attention [3] since its experimental realization in cold atomic gases. By applying counter propagating Raman pulses with tunable properties, the effective gauge field and SOC have been accomplished in ultra-cold gases of both bosons [2, 4–9] and fermions [10, 11]. These experimental achievements add an additional piece to the already versatile toolbox of manipulation of cold atoms, and may help paving a new route toward the realization and investigation on novel quantum states. A considerable amount of theoretical interest has been stimulated in the understanding of the SOC effect in both bosonic [12–20] and fermionic [20–34] systems.

Among these works, one important direction is the study of SOC effect in low dimensionality where many interesting novel quantum states may be present. In particular, a BEC with a half-quantum-angular-momentum vortex may exist in two-dimensional (2D) bosonic system with Rashba SOC [17–19]. In two-component Fermi gases, a topological superfluid is proposed in 2D configuration, and can supports zero-energy Majorana modes which are related to fault tolerant quantum computation [29, 30].

In realistic experiments of ultra-cold atoms, the low-dimensional physics are usually studied in a quasi-low-dimensional configuration, where atoms are strongly confined in one or two spatial dimensions such that the trapping frequencies along these directions dominate all other relevant energy scales in an effective low-dimensional Hamiltonian. In the energy scale of interest, this effective Hamiltonian should catch the same physics as the original Hamiltonian, which usually corresponds to two-body processes in the context of cold atoms as the particle separation is much larger than the range of interatomic interaction. Thus, to write down the correct effective low-dimensional Hamiltonian, one needs to investigate the two-body physics in the quasi-low-dimensional confinement, and express the effective low-dimensional scattering amplitude or the two-body binding energy in terms of the "control parameters", including the three-dimensional (3D) scattering length and the intensity of the confinement. In the absence of SOC, this analysis has been performed for quasi-one-dimensional (1D) [36, 37] and quasi-2D [37, 38] configurations, and leads to the unique feature of confinement-induced resonance [36] and a different renormalization scheme around Feshbach resonances [37, 39]. In the presence of SOC, a discussion of two-body physics within quasi-low-dimensional confinement and a derivation of the effective low-dimensional Hamiltonian is still lack.

In this paper, we investigate two-body scattering process and bound state energy of two-component fermionic atoms in 2D and quasi-2D geometries with a Rashba type SOC. For 2D systems, we find that when the total momentum of two atoms is zero, the 2D inter-atomic scattering amplitude in the low-energy limit will be qualitatively altered by the presence of SOC, rendering a *polynomial* rather than logarithmical decay to zero. For quasi-2D systems with a strong harmonic confinement along the axial z-direction, we obtain analytic expression for the effective 2D scattering amplitude. We also derive the equation for the binding energy of two-atom bound states (dimer), as well as the effective mass of the dimer. We find that the presence of Rashba SOC tends to *enhance* the two-body binding energy. This observation can be qualitatively understood by noticing that the density of states in the low energy limit is increased as the ground state becomes degenerate with SOC. Based on these results, we further derive an effective 2D interaction between atoms in the quasi-2D gas with Rashba SOC, and map out two effective 2D Hamiltonians which are responsive for energy regimes around the two-body binding energy and close to the single-particle threshold. These effective models can be used to study many-body properties of quasi-2D gas with attractive or repulsive interactions, respectively. Our results provide the possibility to control the effective 2D physics via 3D parameters including the scattering length and the intensity of z-confinement. The method developed in this manuscript can be directly generalized to other systems with all kinds of atoms and arbitrary types of SOC.

The remainder of this manuscript is organized as follows. In Sec. II, we discuss the two-body physics in 2D. In Sec. III, we calculate the low-energy scattering amplitude and the binding energy of dimers in a quasi-2D geometry with a strong harmonic trapping potential along the axial z-direction. By matching the two-body physics, we construct in Sec. IV the effective 2D Hamiltonian which can describe the low-energy behavior of the quasi-2D gas. The main results are discussed and summarized in Sec. V, while some details of our calculations are explained in the appendixes.

II. 2D SCATTERING WITH RASHBA SOC

In this section we discuss the scattering and bound states of two spin-1/2 fermionic atoms in a pure-2D geometry (x-y plane) with Rashba SOC. In such a system, the total momentum $\boldsymbol{q}$ of the two atoms is conserved. Then the spatial motion of the mass center of the two atoms is separated from the relative motion and the spin of the two atoms. Thus, the quantum state of the two-atom relative motion can be described by a spinor wave function

$$\begin{aligned}|\psi(\boldsymbol{\rho})\rangle &= \psi_{\uparrow\uparrow}(\boldsymbol{\rho})|\uparrow\rangle_1|\uparrow\rangle_2+\psi_{\uparrow\downarrow}(\boldsymbol{\rho})|\uparrow\rangle_1|\downarrow\rangle_2\\ &\quad+\psi_{\downarrow\uparrow}(\boldsymbol{\rho})|\downarrow\rangle_1|\uparrow\rangle_2+\psi_{\downarrow\downarrow}(\boldsymbol{\rho})|\downarrow\rangle_1|\downarrow\rangle_2 \quad (1)\end{aligned}$$

with $\boldsymbol{\rho}=(x,y)$ the 2D relative coordinate of the two atoms and $|\uparrow\rangle_{1(2)}$ and $|\downarrow\rangle_{1(2)}$ the spin eigen-states of the 1st (2nd) atom. It is apparently that the wave function $|\psi(\boldsymbol{\rho})\rangle$ can also be considered as a $\boldsymbol{\rho}$-dependent spin stae of the two atoms. In this paper, we use the nature unit $\hbar=m=1$ with m the single-atom mass.

Due to the presence of SOC, the relative motion of the two atoms depends on their center-of-mass momentum $\boldsymbol{q}$. For a given value of $\boldsymbol{q}=(q_x,q_y)$, the Hamiltonian for atomic relative motion and spin degrees of freedom is given by

$$H^{(\mathrm{2D})}=H_0^{(\mathrm{2D})}+V_{\mathrm{2D}}(\rho), \quad (2)$$

where the 2D free Hamiltonian $H_0^{(\mathrm{2D})}$ is given by

$$\begin{aligned}H_0^{(\mathrm{2D})} &= -\sum_{\beta=x,y}\frac{\partial^2}{\partial\beta^2}+\frac{\xi}{2}\sum_{j=1,2}\left[\frac{q_x}{2}+(-1)^j p_x\right]\hat{\sigma}_x^{(j)}\\ &\quad+\frac{\xi}{2}\sum_{j=1,2}\left[\frac{q_y}{2}+(-1)^j p_y\right]\hat{\sigma}_y^{(j)} \quad (3)\end{aligned}$$

with $\boldsymbol{p}=(p_x,p_y)$ the relative momentum of the two atoms. The Rashba SOC is described by the second term of Eq. (3), where $\boldsymbol{q}/2+(-1)^j\boldsymbol{p}$ is the momentum of the j-th atom. The spin operator $\hat{\sigma}_{x,y}^{(j)}$ for the j-th atom is defined as $\hat{\sigma}_x^{(j)}=|\uparrow\rangle_j\langle\downarrow|+|\uparrow\rangle_j\langle\downarrow|$ and $\hat{\sigma}_y^{(j)}=-i|\uparrow\rangle_j\langle\downarrow|+i|\downarrow\rangle_j\langle\uparrow|$. Without loss of generality, we assume the SOC intensity ξ in Eq. (3) is a positive real number.

In Eq. (2) $V_{\mathrm{2D}}(\rho)$ is the atom-atom interaction potential with $\rho=|\boldsymbol{\rho}|$. We assume the effective range of the potential $V_{\mathrm{2D}}(\rho)$ is ρ_*, that is the potential becomes negligible in the region $\rho\gtrsim\rho_*$. We further assume the SOC is weak enough so that $\xi\ll 4/\rho_*$.

To investigate the scattering process in our systems, we first define single-atom spin state $|\alpha_j,\boldsymbol{t}\rangle_j$ for the j-th atom as

$$\frac{\xi}{2}\left(t_x\hat{\sigma}_x^{(j)}+t_y\hat{\sigma}_y^{(j)}\right)|\alpha_j,\boldsymbol{t}\rangle_j=\alpha_j\frac{\xi|\boldsymbol{t}|}{2}|\alpha_j,\boldsymbol{t}\rangle_j \quad (4)$$

with $\boldsymbol{t}=(t_x,t_y)$ any 2D vector and $\alpha_j=\pm1$. We further define the two-atom spin state $|\boldsymbol{\alpha}(\boldsymbol{q},\boldsymbol{k})\rangle$ as

$$|\boldsymbol{\alpha}(\boldsymbol{q},\boldsymbol{k})\rangle=|\alpha_1,\frac{\boldsymbol{q}}{2}+\boldsymbol{k}\rangle_1|\alpha_2,\frac{\boldsymbol{q}}{2}-\boldsymbol{k}\rangle_2, \quad (5)$$

with $\boldsymbol{\alpha}=(\alpha_1,\alpha_2)$ and $\bar{\boldsymbol{\alpha}}=(\alpha_2,\alpha_1)$.

In the scattering process, the incident wave function shoud be the eigen-state of the Hamiltonian $H_0^{(\mathrm{2D})}$ for the free motion of the two fermionic atoms. The straightforward calculation shows that the such a incident wave function takes the form

$$|\psi_c^{(0)}(\boldsymbol{\rho})\rangle=\frac{e^{i\boldsymbol{k}\cdot\boldsymbol{\rho}}}{2^{3/2}\pi}|\boldsymbol{\alpha}(\boldsymbol{q},\boldsymbol{k})\rangle-\frac{e^{-i\boldsymbol{k}\cdot\boldsymbol{\rho}}}{2^{3/2}\pi}|\bar{\boldsymbol{\alpha}}(\boldsymbol{q},-\boldsymbol{k})\rangle. \quad (6)$$

with incident momentum $\boldsymbol{k}=(k_x,k_y)$. In this paper we denote

$$c=(\boldsymbol{\alpha},\boldsymbol{q},\boldsymbol{k}) \quad (7)$$

as the set of all the three quantum numbers. Here we have considered the Pauli's principle for the fermonic atoms. The eigen-energy of $H_0^{(\mathrm{2D})}$ with respect to the eigen-state $|\psi_c^{(0)}(\boldsymbol{\rho})\rangle$ is

$$\varepsilon_c=k^2+\frac{\xi}{2}\left(\alpha_1\left|\frac{\boldsymbol{q}}{2}+\boldsymbol{k}\right|+\alpha_2\left|\frac{\boldsymbol{q}}{2}-\boldsymbol{k}\right|\right) \quad (8)$$

with $k=|\boldsymbol{k}|$. Notice that in the presence of SOC, the scattering threshold, or the minimum value of ε_c with respect to a fixed $\boldsymbol{q}$, is shifted from 0 to $\varepsilon_{\mathrm{thre}}(q)$ which is given by

$$\varepsilon_{\mathrm{thre}}(q)=\begin{cases}-q^2/4-\xi^2/4 & (q<\xi)\\ -q\xi/2 & (q>\xi)\end{cases} \quad (9)$$

with $q=|\boldsymbol{q}|$.

Now we consider the scattering state $|\psi_c^{(+)}(\boldsymbol{\rho})\rangle$ with respect to the incident state $|\psi_c^{(0)}(\boldsymbol{\rho})\rangle$. We assume the scattering energy ε_c is low enough with $k\ll 1/\rho_*$. In such a low-energy case and within the region of $\rho \gtrsim \rho_*$, the wave function of the scattering state $|\psi_c^{(+)}(\boldsymbol{\rho})\rangle$ can be expressed as (see discussion in Appendix A and in Ref. [38])

$$|\psi_c^{(+)}(\boldsymbol{\rho})\rangle \approx |\psi_c^{(0)}(\boldsymbol{\rho})\rangle + A(c)\, g(\varepsilon_c; \boldsymbol{\rho}, \mathbf{0})\, |0,0\rangle, \tag{10}$$

where

$$|0,0\rangle = 1/\sqrt{2}\left(|\uparrow\rangle_1 |\downarrow\rangle_2 - |\downarrow\rangle_1 |\uparrow\rangle_2\right) \tag{11}$$

is the spin singlet state, and the 2D free Green's function $g(\eta; \boldsymbol{\rho}, \boldsymbol{\rho}')$ is given by

$$g(\eta; \boldsymbol{\rho}, \boldsymbol{\rho}') = \frac{1}{\eta + i0^+ - H_0^{(2\mathrm{D})}} \delta(\boldsymbol{\rho} - \boldsymbol{\rho}'), \tag{12}$$

and can be considered as a $(\boldsymbol{\rho}, \boldsymbol{\rho}')$-dependent operator for the two-atom spin.

The coefficient $A(c)$ in Eq. (10) can be derived with the following analysis. First, it can be proved (see Appendix B) that in the *small-distance region* $\rho_* \lesssim \rho \ll 1/k$ the function $|\psi^{(c,+)}(\boldsymbol{\rho})\rangle$ behaves as

$$|\psi^{(c,+)}(\boldsymbol{\rho})\rangle \propto (\ln \rho - \ln d)\, |0,0\rangle \tag{13}$$

Here, the $\boldsymbol{\rho}$-independent factor $\ln d$ is determined by ξ and the detail of the potential $V_{2\mathrm{D}}(\rho)$ (Appendix B). and almost independent on the scattering energy ε_c in the low-energy case [38]. Second, the calculations in Appendix C shows that, in the small-distance region we have

$$\begin{aligned}\langle 0,0|g(\eta; \boldsymbol{\rho}, \mathbf{0})|0,0\rangle \approx\ & \frac{1}{2\pi}\left[\ln \rho + C + \ln\left(-i\frac{\sqrt{\varepsilon_c}}{2}\right)\right] \\ & + \lambda(\varepsilon_c, \boldsymbol{q})\end{aligned} \tag{14}$$

where $C = 0.5772...$ is the Euler gamma number and the function $\lambda(\eta, \boldsymbol{q})$ is defined as

$$\begin{aligned}\lambda(\eta, \boldsymbol{q}) = & \frac{1}{(2\pi)^2} \sum_{\boldsymbol{\alpha}''} \int d\boldsymbol{k}'' \left|\langle 00|\boldsymbol{\alpha}''(\boldsymbol{q}, \boldsymbol{k}'')\rangle\right|^2 \times \\ & \left(\frac{1}{\eta + i0^+ - \varepsilon_{c''}} - \frac{1}{\eta + i0^+ - |\boldsymbol{k}''|^2}\right),\end{aligned} \tag{15}$$

with $c'' = (\boldsymbol{\alpha}''; \boldsymbol{q}; \boldsymbol{k}'')$. For $\boldsymbol{q} = 0$, a straightforward calculation shows that the function $\lambda(\eta, \mathbf{0})$ can be further simplified as

$$\lambda(\eta, \mathbf{0}) = \frac{1}{2(2\pi)} \times \\ \begin{cases} \frac{-\xi}{2\sqrt{-4\eta-\xi^2}}\left(\pi + 2\arctan\left[\frac{\xi^2+2\eta}{\xi\sqrt{-4\eta-\xi^2}}\right]\right); (\eta < -\frac{\xi^2}{4}) \\ \frac{-i\pi\xi}{2\sqrt{\eta+\xi^2/4}} + \xi\frac{\operatorname{arctanh}\left(2\sqrt{\eta+\xi^2/4}/\xi\right)}{\sqrt{\eta+\xi^2/4}}; (-\frac{\xi^2}{4} < \eta < 0) \\ \frac{\xi}{\sqrt{\eta+\xi^2/4}}\operatorname{arctanh}\frac{\xi}{2\sqrt{\eta+\xi^2/4}}; (0 < \eta < 1 - \frac{\xi^2}{4}) \end{cases} . \tag{16}$$

Substituting Eq. (14) into (10), we get the expression for $|\psi_c^{(+)}(\boldsymbol{\rho})\rangle$ in the small-distance region

$$\begin{aligned}& |\psi_c^{(+)}(\boldsymbol{\rho})\rangle \approx |\psi_c^{(0)}(\boldsymbol{\rho})\rangle + \\ & \frac{A(c)}{2\pi}\left\{\ln \rho + C + \ln\left(-\frac{i\sqrt{\varepsilon_c}}{2}\right) + \lambda[\varepsilon_c, \boldsymbol{q}]\right\}|0,0\rangle .\end{aligned} \tag{17}$$

Comparing Eqs. (17) and (13), we obtain the expression for the parameter $A(c)$:

$$A(c) = \frac{(2\pi)\langle 0,0|\psi_c^{(0)}(\mathbf{0})\rangle}{i\pi/2 - C - \ln\left(d\sqrt{\varepsilon_c}/2\right) - (2\pi)\lambda(\varepsilon_c, \boldsymbol{q})}. \tag{18}$$

According to Eq. (10), $A(c)$ completely determines the behavior of the scattering-state wave function $|\psi^{(c,+)}(\boldsymbol{\rho})\rangle$ in the region of $\rho \gtrsim \rho_*$.

According to scattering theory [42], we can define the 2D scattering amplitude $f^{(2\mathrm{D})}$ between the incident state $|\psi_c^{(0)}(\boldsymbol{\rho})\rangle$ and an energy-conserved output state $|\psi_{c'}^{(0)}(\boldsymbol{\rho})\rangle$ with $\boldsymbol{q}' = \boldsymbol{q}$ and $\varepsilon_c = \varepsilon_{c'}$ as

$$f^{(2\mathrm{D})}(c' \leftarrow c) = -2\pi^2 \int d\boldsymbol{\rho} \langle \psi_{c'}^{(0)}(\boldsymbol{\rho})|V_{2\mathrm{D}}|\psi_c^{(+)}(\boldsymbol{\rho})\rangle. \tag{19}$$

A straightforward calculation (Appendix D) shows that we can express $f^{(2\mathrm{D})}$ in terms of the coefficient $A(c)$

$$f^{(2\mathrm{D})}(c' \leftarrow c) = -2\pi^2 \langle \psi_{c'}^{(0)}(\mathbf{0})|0,0\rangle A(c). \tag{20}$$

Now we discuss the two-body bound states with Rashba SOC in two-dimensions, as is also investigated in Ref. [34]. As shown in Appendix A, when the energy ε_b of the bound state is close enough to the scattering threshold $\varepsilon_{\mathrm{thre}}(q)$, or the condition $\varepsilon_{\mathrm{thre}}(q) - \varepsilon_b \ll 1/\rho_*^2$ is satisfied, the wave function $|\psi_b(\boldsymbol{\rho})\rangle$ of the two-atom bound state can be approximated as

$$|\psi_b(\boldsymbol{\rho})\rangle \approx B g(\varepsilon_b; \boldsymbol{\rho}, \mathbf{0})\, |0,0\rangle \tag{21}$$

in the region $\rho \gtrsim \rho_*$. Here, B is the normalization coefficient and g is defined in Eq. (12). The energy ε_b of the bound state is determined by the condition (appendix B)

$$\langle 0,0|\psi_b(\boldsymbol{\rho})\rangle \propto \ln \rho - \ln d \tag{22}$$

in the region $\rho_* \lesssim \rho \ll 1/\sqrt{|\varepsilon_b - \varepsilon_{\mathrm{thre}}(q)|}$, or by the equation

$$-\ln d = C + \ln\left(-\frac{i\sqrt{\varepsilon_b}}{2}\right) + (2\pi)\,\lambda(\varepsilon_b, \boldsymbol{q}). \tag{23}$$

Here, we use the fact that in the small-distance region the function $\langle 0,0|g(\varepsilon_b; \boldsymbol{\rho}, \mathbf{0})|0,0\rangle$ also takes the form as in Eq. (14), with ε_c replaced by the new variable ε_b. Therefore, the bound-state energy ε_b is a function of both the characteristic length d and the center-of-mass momentum $\boldsymbol{q}$.

In the discussion above, we obtain the analytical expressions for the scattering amplitude $f^{(2\mathrm{D})}$ and the equation for the bound-state energy in a pure 2D geometry

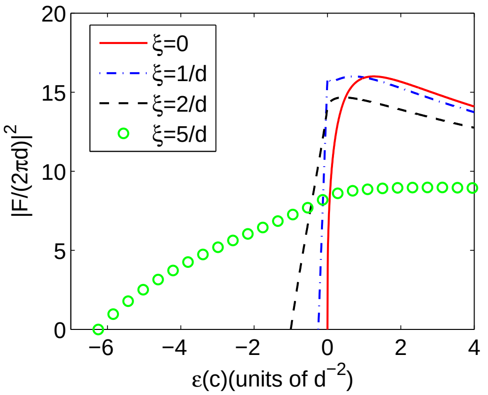

FIG. 1: (Color online) The variation of function $|F|^2$ with 2D scattering energy $\varepsilon(c)$. Here, F is defined in Eq. (26) and d is the parameter in Eq. (13). We show results in cases with zero center-of-mass momentum $q = 0$ and SOC intensity $\xi = 0$ (red solid line), $1/d$ (blue dashed-dotted line), $2/d$ (black dashed line) and $5/d$ (green open circle).

with Rashba SOC. Comparing our results with the 2D scattering theory without SOC (see Appendix E and Ref. [38]), we observe the following two qualitative differences:

First, when the total momentum $\boldsymbol{q}$ of the two atoms is zero, the SOC changes the dependence of the scattering amplitudes on the scattering energy ε_c. As shown in Appendix E, when there is no SOC, the scattering amplitude $f_0^{(2\mathrm{D})}$ decays to zero logarithmically in the limit $\varepsilon_c \to 0$,

$$\lim_{\varepsilon_c \to 0} f_0^{(2\mathrm{D})} \propto \frac{1}{\ln \varepsilon_c}. \qquad (24)$$

When $\boldsymbol{q} = 0$, a Rashba SOC will change the scattering amplitude through the function $\lambda\left(\varepsilon_c, \mathbf{0}\right)$ in $A\left(c\right)$ and the factor $\langle \psi_{c'}^{(0)}\left(\mathbf{0}\right)|0,0\rangle\langle 0,0|\psi_c^{(0)}\left(\mathbf{0}\right)\rangle$. In particular, the λ-function removes the logarithmic behavior of the scattering amplitude in the region around $\varepsilon_c = 0$, leading to

$$\lim_{\varepsilon_c \to -\xi^2/4} f^{(2\mathrm{D})} \propto \sqrt{\varepsilon_c + \frac{\xi^2}{4}}. \qquad (25)$$

Namely, in the presence of Rashba SOC, the scattering amplitude $f^{(2\mathrm{D})}$ polynomially decays to zero in the limit of $\varepsilon_c \to -\xi^2/4$.

To illustrate the SOC effect to the 2D scattering amplitude, we plot in Fig. 1 the mode square of the quantity

$$F \equiv \frac{f^{(2\mathrm{D})}\left(c' \leftarrow c\right)}{\langle \psi_{c'}^{(0)}\left(\mathbf{0}\right)|0,0\rangle\langle 0,0|\psi_c^{(0)}\left(\mathbf{0}\right)\rangle} \qquad (26)$$

as a function of the scattering energy ε_c with respect to different SOC intensities. It can be seen clearly that the function $|F|^2$ linearly decays to zero in the limit of $\varepsilon_c \to -\xi^2/4$ in the presence of SOC, and logarithmically decays to zero when there is no SOC.

We emphasize that, this change is due to the dispersive relation (8) of ε_c. When $\boldsymbol{q} = 0$, ε_c is independent of the direction of $\boldsymbol{k}$, and takes minimum value $-\xi^2/4$ when $k = \xi/2$. Namely, we have $\varepsilon_c = -\xi^2/4$ for all momenta $\boldsymbol{k}$ in the circle of (k_x, k_y) plane. Nevertheless, when $\boldsymbol{q} \neq 0$, or when SOC is not of Rashba type, this character disappears. In these cases ε_c takes minimum value only when $\boldsymbol{k}$ takes one or two certain values, as in the systems without SOC. Thus, the 2D scattering amplitude also logarithmically decays to zero when the scattering energy approaches to the threshold.

Second, when there is no SOC, the scattering amplitude is independent on the center-of-mass momentum $\boldsymbol{q}$. This feature is qualitatively altered by the presence of SOC, as can be clearly seen from Eq. (3) where the SOC terms couple the relative motion of the two atoms with the total momentum $\boldsymbol{q}$. As a consequence, the scattering amplitude $f^{(2\mathrm{D})}$ becomes a function of $\boldsymbol{q}$. The similar $\boldsymbol{q}$-dependence can also be observed in the bound-state energy ε_b of the low-energy bound states [34].

III. SCATTERING IN A QUASI-2D CONFINEMENT WITH RASHBA SOC

In the previous section, we obtain the two-atom scattering amplitude and bound-state energy in a pure 2D system with Rashba SOC. Our results show that the SOC qualitatively changes the 2D scattering amplitude. In a realistic experiment of cold atoms, the 2D condition is usually realized by applying a tight confinement along one (say z) direction, such that the degrees of freedom of the single-body Hamiltonian along that specific direction can be approximately integrated out. In this section, we study the scattering and bound states of two spin-1/2 fermionic atoms in a quasi-2D configuration. We conclude that the qualitative effects introduced by Rashba SOC to the two-body physics in pure 2D geometry also exist in the quasi-2D cases. Besides, we show how the factor $\ln d$ in the expressions of 2D scattering amplitude and bound state energy can be effectively tuned by the atomic 3D scattering length and the intensity of z-confinement.

A. System and Hamiltonian

We consider a quasi-2D configuration with a harmonic trap with frequency ω applied along the z-direction, while the atomic motion in the x-y plane is free. In the quasi-2D case, the total momentum $\boldsymbol{q}$ of the two atoms in the x-y plane is also conserved and serves as a parameter for the atomic relative motion, as in the pure 2D case. For a given value of $\boldsymbol{q}$, the Hamiltonian of the atomic relative motion and spin states takes the form

$$H = H_0^{(2\mathrm{D})} + H_z + V_{3\mathrm{D}}\left(r\right). \qquad (27)$$

Here, $H_0^{(2\mathrm{D})}$ is defined in Eq. (3),

$$H_z = -\frac{\partial^2}{\partial z^2} + \frac{\omega^2 z^2}{4} - \frac{\omega}{2} \tag{28}$$

is the Hamiltonian for the two-atom relative motion in the z-direction, with z the relative coordinate of the two atoms in this direction. Note that we have shifted the zero-energy point for our convenience, since the harmonic confinement allows us to separate the relative motion in the z-direction from the center-of-mass degree of freedom.

In Eq. (27), the atom-atom interaction potential $V_{3\mathrm{D}}\left(r\right)$ is a function of the relative position $\boldsymbol{r} = (\boldsymbol{\rho}, z) = (x, y, z)$ of the two atoms in three dimensions. Here, we have $r = |\boldsymbol{r}|$ and denote the effective range of $V_{3\mathrm{D}}\left(r\right)$ as r_*. In the region $r \gtrsim r_*$, the potential $V_{3\mathrm{D}}\left(r\right)$ becomes negligible. For simplicity, we further assume $V_{3\mathrm{D}}\left(r\right)$ is independent on the atomic spin, and consider only the weak SOC case with $4/\xi \gg r_*$.

B. Two-atom scattering state

In the quasi-2D configuration, we consider only the scattering between two fermionic atoms in the ground state of H_z. Then the incident wave function is given by

$$|\Psi_c^{(0)}\left(\boldsymbol{r}\right)\rangle = \varphi_0\left(z\right)|\psi_c^{(0)}\left(\boldsymbol{\rho}\right)\rangle \tag{29}$$

with $|\psi_c^{(0)}\left(\boldsymbol{\rho}\right)\rangle$ defined in Eq. (6). Here, $\varphi_{n_z}\left(z\right)$ is the n_z-th eigen-wave function of H_z. Without loss of generality, we set the phase of $\varphi_{n_z}\left(z\right)$ so that $\varphi_{n_z}\left(0\right)$ is real. We further assume the energy gap between the incident state and the threshold $\varepsilon_{\mathrm{thre}}$ is smaller than the trapping frequency along the z-direction, i.e. $|\varepsilon_c - \varepsilon_{\mathrm{thre}}(q)| < \omega$. In this case, the energy-conserved output states of the scattering are also in the ground transverse channel with $\varphi_0\left(z\right)$.

Next, we calculate the scattering state $|\Psi_c^{(+)}\left(\boldsymbol{r}\right)\rangle$ with respect to the incident state $|\Psi_c^{(0)}\left(\boldsymbol{r}\right)\rangle$. The scattering state can be obtained with the same method as in Sec. II. As shown in appendix A and Ref. [38], in the region of $r \gtrsim r_*$, the scattering state wave function $|\Psi_c^{(+)}\left(\boldsymbol{r}\right)\rangle$

$$|\Psi_c^{(+)}\left(\boldsymbol{r}\right)\rangle \approx |\Psi_c^{(0)}\left(\boldsymbol{r}\right)\rangle + \frac{A_{\mathrm{eff}}\left(c\right)}{\varphi_0\left(0\right)} G(\varepsilon_c; \boldsymbol{r}, \boldsymbol{0})|0,0\rangle, \tag{30}$$

with the quasi-2D free Green's function $G\left(\eta; \boldsymbol{\rho}, \boldsymbol{\rho}'\right)$ given by

$$G\left(\eta; \boldsymbol{r}, \boldsymbol{r}'\right) = \frac{1}{\eta + i0^+ - \left[H_0^{(2\mathrm{D})} + H_z\right]} \delta\left(\boldsymbol{r} - \boldsymbol{r}'\right). \tag{31}$$

Here $A_{\mathrm{eff}}\left(c\right)$ is a $\boldsymbol{r}$-independent coefficient, and can be derived with the following two facts. First, it can be proved (see Appendix B) that in the small-distance region $r_* \lesssim r \ll 1/k$ the function $|\Psi_c^{(+)}\left(\boldsymbol{r}\right)\rangle$ behaves as

$$\langle 0,0|\Psi_c^{(+)}\left(\boldsymbol{r}\right)\rangle \propto \left(\frac{1}{r} - \frac{1}{a}\right) \tag{32}$$

with a the s-wave scattering length determined by ξ and the detail of $V_{3\mathrm{D}}\left(r\right)$ (Appendix B). Second, Appendix C also shows that, in the small-distance region we have

$$\begin{aligned}\langle 0,0|G(\eta; \boldsymbol{r}, \boldsymbol{0})|0,0\rangle \approx & -\frac{1}{4\pi r} - \frac{w\left(\frac{\varepsilon_c}{2\omega}\right)}{2\left(2\pi\right)^{3/2} l_0} \\ & + \sum_{n_z=0}^{\infty} |\varphi_{n_z}(0)|^2 \lambda(\varepsilon_c - n_z\omega; \boldsymbol{q}),\end{aligned} \tag{33}$$

where $l_0 = \sqrt{1/\omega}$, $w\left(\eta\right)$ is defined as

$$\begin{aligned} & w\left(\eta\right) = \\ & \lim_{N\to\infty} \left(2\sqrt{\frac{N}{\pi}} \ln\frac{N}{e^2} - \sum_{j=0}^{N} \frac{(2j-1)!!}{(2j)!!} \ln\left(j - \eta - i0^+\right)\right)\end{aligned} \tag{34}$$

and $\lambda(\eta; \boldsymbol{q})$ is defined in Eq. (15). Substituting Eqs. (30) and (33) into (32), we can obtain the parameter $A_{\mathrm{eff}}\left(c\right)$. We find that $A_{\mathrm{eff}}\left(c\right)$ can be formally expressed as in Eq. (18), with the 2D effective range d replaced by a quasi-2D effective range d_{eff}

$$\begin{aligned} & A_{\mathrm{eff}}\left(c\right) = \\ & \frac{\left(2\pi\right)\langle 0,0|\psi_c^{(0)}\left(\boldsymbol{0}\right)\rangle}{i\pi/2 - C - \ln\left\{d_{\mathrm{eff}}\left(\varepsilon_c, \boldsymbol{q}\right)\sqrt{\varepsilon_c}/2\right\} - \left(2\pi\right)\lambda\left(\varepsilon_c, \boldsymbol{q}\right)}.\end{aligned} \tag{35}$$

Here, the effective characteristic length d_{eff} is a function of the scattering energy ε_c, the center-of-mass momentum $\boldsymbol{q}$, and the 3D scattering length a, and can be determined by

$$\begin{aligned}\ln d_{\mathrm{eff}}\left(\varepsilon_c, \boldsymbol{q}\right) = & -\frac{\sqrt{2\pi} w\left(\frac{\varepsilon_c}{2\omega}\right)}{2} - \ln\left(-\frac{i\sqrt{\varepsilon_c}}{2}\right) - C \\ & -\frac{\pi l_0}{a} + \left(2\pi\right)^2 l_0 \sum_{n_z=1}^{\infty} |\varphi_{n_z}\left(0\right)|^2 \lambda(\varepsilon_c - n_z\omega; \boldsymbol{q}).\end{aligned} \tag{36}$$

Note that the summation of n_z on the right-hand-side of Eq. (36) runs over all natural numbers. One can easily show that $\ln d_{\mathrm{eff}}\left(\eta, \boldsymbol{q}\right)$ always takes a real value when $\eta < \varepsilon_{\mathrm{thre}}(\boldsymbol{q}) + \omega$. We would like to emphasize that the term $\ln d_{\mathrm{eff}}$ governs the effective 2D physics in this quasi-2D system, and includes all effects given by the control parameters a and ω.

C. Effective 2D scattering amplitude

The straightforward calculation shows that, in the region $\rho \gg l_0$ we have

$$|\Psi_c^{(+)}\left(\boldsymbol{r}\right)\rangle \approx \varphi_0\left(z\right)\left(|\psi_c^{(0)}\left(\boldsymbol{\rho}\right)\rangle + A_{\mathrm{eff}}\left(c\right) g\left(\varepsilon_c; \boldsymbol{\rho}, \boldsymbol{0}\right)|0,0\rangle\right), \tag{37}$$

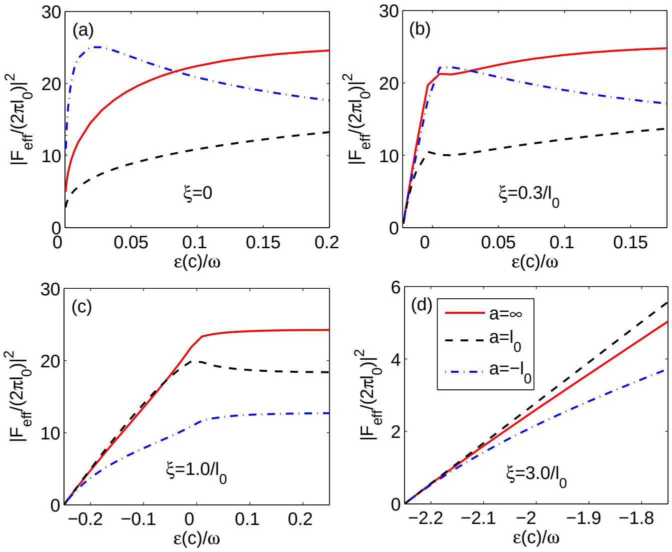

FIG. 2: (Color online) The variation of $|F_{\rm eff}|^2$ as functions of the quasi-2D scattering energy $\varepsilon(c)$. Here, $F_{\rm eff}$ is defined in Eq. (40) and $l_0 = 1/\sqrt{\omega}$. We show the results with zero center-of-mass momentum $q = 0$, SOC intensities $\xi =$ (a) 0, (b) $0.3/l_0$, (c) $1/l_0$, (d) $3/l_0$ and 3D scattering lengths $a = \infty$ (red solid line), l_0 (black dashed line) and $-l_0$ (blue dashed-dotted line).

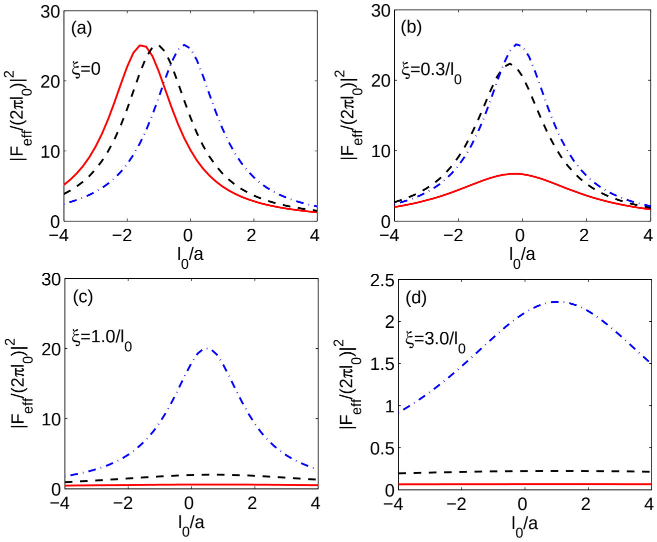

FIG. 3: (Color online) The variation of $|F_{\rm eff}|^2$ with 3D scattering length. The function $F_{\rm eff}$ is defined in Eq. (40) and $l_0 = 1/\sqrt{\omega}$. We show the results with zero center-of-mass momentum $q = 0$, SOC intensities $\xi =$ (a) 0, (b) $0.3/l_0$, (d) $1/l_0$, (d) $3/l_0$ and the quasi-2D scattering energy $\varepsilon(c) = -\xi^2/4 + 0.006\omega$ (red solid line), $-\xi^2/4 + 0.02\omega$ (black dashed line) and $-\xi^2/4 + 0.2\omega$ (blue dashed-dotted line).

where the 2D Green's function g is defined in Eq. (12). Comparing Eq. (37) and Eq. (10), we find that in the long-range region with $\rho \gg l_0$, the quasi-2D scattering state wave function $|\Psi_c^{(+)}(\boldsymbol{r})\rangle$ is the product of $\varphi_0(z)$ and a 2D scattering-state wave function. Therefore, if we focus on the long-range region, the quasi-2D scattering process is equivalent to a 2D scattering process with an effective characteristic length $d_{\rm eff}(\varepsilon_c, \boldsymbol{q})$, which is controlled by the 3D scattering length a and the trapping frequency ω in the z-direction.

The quasi-2D scattering amplitude between the incident state $|\Psi_c^{(0)}(\boldsymbol{r})\rangle$ and an energy-conserved output state $|\Psi_{c'}^{(0)}(\boldsymbol{r})\rangle$ with $\boldsymbol{q} = \boldsymbol{q}'$ and $\varepsilon_{c'} = \varepsilon_c$ is defined as

$$f^{(2D)}(c' \leftarrow c) = -2\pi^2 \int d\boldsymbol{r}' \langle \Psi_{c'}^{(0)}(\boldsymbol{r}') \,|\, V_{3D}(r') \,|\Psi_c^{(+)}(\boldsymbol{r}')\rangle. \tag{38}$$

As shown in appendix D, $f^{(Q2D)}(c' \leftarrow c)$ can be expressed as

$$f^{(Q2D)}(c' \leftarrow c) = -2\pi^2 \langle \psi_{c'}^{(0)}(\mathbf{0}) | 0, 0\rangle A_{\rm eff}(c). \tag{39}$$

Comparing Eq. (39) with (20), we find that $f^{(Q2D)}$ is nothing but the 2D scattering amplitude with respect to the 2D scattering state given by the right-hand side of Eq. (37).

To understand the behavior of the effective quasi-2D scattering amplitude $f^{(Q2D)}$, we show in Figs. 2 and 3 the variation of the mode square of the function

$$F_{\rm eff} \equiv \frac{f^{(Q2D)}(c' \leftarrow c)}{\langle \psi_{c'}^{(0)}(\mathbf{0}) | 0, 0\rangle \langle 0, 0 | \psi_c^{(0)}(\mathbf{0})\rangle} \tag{40}$$

with scattering energy ε_c, SOC intensity ξ, 3D scattering length a and characteristic length l_0 of the z-confinement. In Fig. 2, it is shown clearly that the quantity $|F_{\rm eff}|^2$ linearly decays to zero in the low-energy limit $\varepsilon_c \to \varepsilon_{\rm thre}(q)$ with SOC, and logarithmically decays to zero when there is no SOC. This observation is consistent with the outcome in the pure 2D systems as discussed in the previous section. In Fig. 3 we investigate the behavior of $|F_{\rm eff}|^2$ as functions of the scattering length for different values of $\varepsilon_c - \varepsilon_{\rm thre}(q)$. Note that for a given value of $\varepsilon_c - \varepsilon_{\rm thre}(q)$, the resonance behavior of $|F_{\rm eff}|^2$ is still maintained, while the resonance point is shifted by the SOC and the amplitude of $|F_{\rm eff}|^2$ is suppressed by the SOC.

D. Two-atom bound state

Next, we consider the two-body bound state in quasi-2D configuration. Similar as in Sec. II, it can be shown that in the region $r \gtrsim r_*$ the wave function $|\Psi_b(\boldsymbol{r})\rangle$ can be expressed as

$$|\Psi_b(\boldsymbol{r})\rangle = B' G(E_b; \boldsymbol{r}, \mathbf{0}) |0, 0\rangle \tag{41}$$

with B' the normalization factor. In the long-range limit $r \gg l_0$, the wave function of the quasi-2D bound state is proportional to that of the pure-2D bound state in Eq. (21). The energy E_b of the quasi-2D bound state is determined by the boundary condition in the small-distance region (appendix B)

$$\langle 0, 0 | \Psi_b(\boldsymbol{r})\rangle \propto \frac{1}{r} - \frac{1}{a} \tag{42}$$

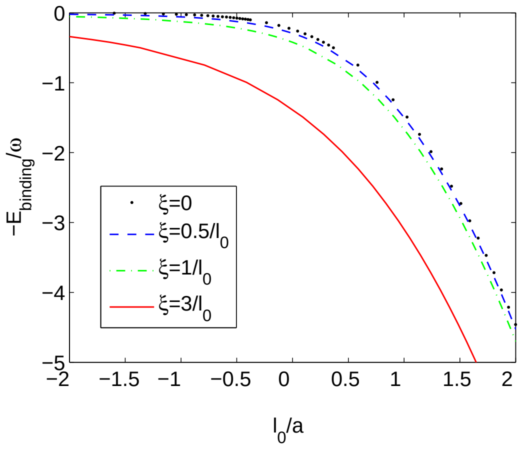

FIG. 4: (Color online) The binding energy $E_{\mathrm{binding}} = \varepsilon_{\mathrm{thre}}(q) - E_b$ of the quasi-2D two-atom bound state as a function of the 3D scattering length. In this plot, we set the center-of-mass momentum $q = 0$ and the SOC intensities $\xi = 0$ (black dots), $0.5/l_0$ (blue dashed line), $1/l_0$ (green dashed-dotted line) and $3/l_0$ (red solid line).

Then it is easy to prove that the boundary condition Eq. (42) is equivalent to the equation

$$-\ln d_{\mathrm{eff}}\left(E_b, \boldsymbol{q}\right) = C + \ln\left(-\frac{i\sqrt{E_b}}{2}\right) + 2\pi\lambda(E_b, \boldsymbol{q}). \tag{43}$$

In Fig. 4, we show the behavior of binding energy

$$E_{\mathrm{binding}} = \varepsilon_{\mathrm{thre}}(q) - E_b \tag{44}$$

with varying 3D scattering length a and SOC intensity for cases of $q = 0$. Notice that the variation of E_{binding} in terms of $1/a$ has the same qualitative behavior with or without SOC, and the value of E_{binding} is increased with the SOC intensity ξ.

Next, we discuss the dispersion relation of the two-atom bound state. To this end, we express E_b as $E_b = \sum_{n=0}^{\infty} E_{bn} q^n h_n\left(\boldsymbol{q}/q\right)$ and then substitute this expression into Eq. (43). Expanding both sides of Eq. (43), we can obtain all the coefficients E_{bn} and the functions h_n. When q is small, we have

$$E_b \approx E_{b0} + E_{b2} q^2 \tag{45}$$

with E_{b0} and E_{b2} determined by the equations

$$\begin{aligned}\frac{l_0\sqrt{2\pi}}{2a} &= (2\pi)^{3/2} l_0 \sum_{n_z=0}^{\infty} \left|\varphi_{n_z}\left(0\right)\right|^2 \lambda_0(E_{b0} - n_z\omega) \\ &\quad -\frac{1}{2} w\left(\frac{E_{b0}}{2\omega}\right);\end{aligned} \tag{46}$$

and

$$E_{b2} = \frac{\sum_{n_z=0}^{\infty} \left|\varphi_{n_z}\left(0\right)\right|^2 \lambda_2(E_{b0} - n_z\omega)}{\frac{1}{4(2\pi)^{3/2}\omega l_0} w'\left(\frac{E_{b0}}{2\omega}\right) - \sum_{n_z=0}^{\infty} \left|\varphi_{n_z}(0)\right|^2 \lambda_0'(E_{b0} - n_z\omega)}. \tag{47}$$

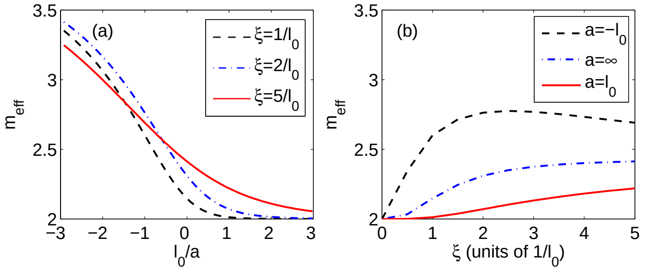

FIG. 5: (Color online) (a) The variation of the effective mass m_{eff} of the two-atom bound state in the quasi-2D system as a function of the 3D scattering length. The SOC intensities used in this plot are $\xi = 1/l_0$ (black dashed line), $2/l_0$ (blue dashed-dotted line) and $5/l_0$ (red solid line). (b) The variation of m_{eff} as a function of the SOC intensity ξ. The 3D scattering lengths used in this plot are $a = -l_0$ (black dashed line), ∞ (blue dashed-dotted line) and l_0 (red solid line).

Here, the functions $\lambda_0\left(\eta\right)$ and $\lambda_2(\eta)$ are defined as

$$\lambda_0\left(\eta\right) = -\frac{\xi\left(\pi + 2\arctan\left[\frac{\xi^2+2\eta}{\xi\sqrt{-4\eta-\xi^2}}\right]\right)}{8\pi\sqrt{-4\eta - \xi^2}} \tag{48}$$

and

$$\begin{aligned}&\lambda_2\left(\eta\right) \\ &= \frac{\xi\left(\xi\sqrt{-4\eta-\xi^2} + 2(2\eta+\xi^2)\arctan\left[\frac{\xi}{\sqrt{-4\eta-\xi^2}}\right]\right)}{32\pi\eta\left(-4\eta-\xi^2\right)^{3/2}}\end{aligned} \tag{49}$$

with $w'\left(\eta\right) = dw\left(\eta\right)/d\eta$ and $\lambda_0'(\eta) = d\lambda_0\left(\eta\right)/d\eta$.

The total energy of the two-body bound state can then be obtained by adding Eq. (45) and the kinetic energy of the center-of-mass motion, leading to $E_{bt} \approx E_{b0} + E_{b2}q^2 + q^2/4$. This quantity can also be expressed in terms of the effective mass

$$m_{\mathrm{eff}} = \frac{1}{2E_{b2} + 1/2}, \tag{50}$$

and takes the form

$$E_{b2} \approx E_{b0} + \frac{q^2}{2m_{\mathrm{eff}}}. \tag{51}$$

In Fig. 5, we plot the effective mass with the 3D scattering length and the SOC intensity.

IV. EFFECTIVE 2D HAMILTONIAN

With the above knowledge of two-body physics, we can construct the effective 2D Hamiltonian for a two-component Fermi gas with Rashba SOC in a quasi-2D confinement. The effective Hamiltonian is required to give the same scattering amplitude or two-body bound state as the original Hamiltonian. It is pointed out that, for each effective 2D Hamiltonian, this criteria can only be satisfied for a small energy range. Thus, in principle one needs to derive different effective Hamiltonian for different energy regions.

We first consider gases with atoms in the low-energy scattering states i.e., the system given by the directly cooling of the atoms with a fixed scattering length. In such a system, the energy of relative motion of two atoms is slightly above $-\xi^2/4$, and the probability for atoms in the excited states along the z-direction is negligible. The atom-atom interaction can be described by a 2D single-channel contact potential

$$\hat{V}_o = \frac{1}{\mathcal{S}} \sum_{\boldsymbol{k},\boldsymbol{k}',\boldsymbol{k}''} {}' g(\boldsymbol{k}+\boldsymbol{k}') a^{\dagger}_{\boldsymbol{k},\uparrow} a^{\dagger}_{\boldsymbol{k}',\downarrow} a_{\boldsymbol{k}'+\boldsymbol{k}'',\downarrow} a_{\boldsymbol{k}'-\boldsymbol{k}'',\uparrow}. \quad (52)$$

Here, $a^{\dagger}_{\boldsymbol{p},\sigma}$ and $a_{\boldsymbol{p},\sigma}$ are the 2D creation and annihilation operators for an atom with momentum $\boldsymbol{p}$ and spin σ, $\mathcal{S}$ is the area of the system, and the summation $\sum'_{\boldsymbol{k},\boldsymbol{k}',\boldsymbol{k}''}$ is done for $|\boldsymbol{k}-\boldsymbol{k}'|/2 < k_c$ and $|(\boldsymbol{k}-\boldsymbol{k}')/2+\boldsymbol{k}''| < k_c$, with k_c a cut-off momentum. For systems without SOC, the coupling intensity $g(\boldsymbol{q})$ is given by the renormalization relation [40] $1/(2\pi g) = -\int_{k<k_c} d\boldsymbol{k}(E_b+k^2)^{-1}$, with E_b the bound-state energy. For our current systems with Rashba SOC, the renormalization relation should be modified as

$$\ln k_c - \frac{1}{2\pi g(\boldsymbol{q})} = -C - \ln\left[\frac{d_{\text{eff}}\left(-\frac{\xi^2}{4},\boldsymbol{q}\right)}{2}\right] \quad (53)$$

with the effective characteristic length d_{eff} defined in Eq. (36). According to the definition, d_{eff} also depends on 3D scattering length a and the characteristic length l_0 of the z confinement. A straightforward calculation (Appendix F) shows that the 2D scattering amplitude given by the interaction potential V_o is the same as the quasi-2D scattering amplitude $f^{(\text{Q2D})}$ as in Eq. (39).

Now we consider the systems with atoms in the bound states. In that case, if the binding energy of the bound state is large, the atomic population in the transverse excited states $\varphi_{n_z}(z)$ with $n_z > 0$ becomes significant [37, 41]. To take into account these transverse excitations, we use a phenomenological two-channel model to describe the atom-atom interaction:

$$\begin{aligned}\hat{V}_b &= \hat{V}_o + \sum_{\boldsymbol{q}}\left(\frac{q^2}{4}+v(\boldsymbol{q})\right) b^{\dagger}_{\boldsymbol{q}} b_{\boldsymbol{q}} \\ &\quad + \frac{1}{\sqrt{\mathcal{S}}}\sum_{\boldsymbol{k},\boldsymbol{k}'} {}' u(\boldsymbol{k}+\boldsymbol{k}') a^{\dagger}_{\boldsymbol{k},\uparrow} a^{\dagger}_{\boldsymbol{k}',\downarrow} b_{\boldsymbol{k}+\boldsymbol{k}'} + h.c. \quad (54)\end{aligned}$$

Here, the open-channel interaction $\hat{V}_o$ is defined as in Eq. (52), $b^{\dagger}_{\boldsymbol{q}}$ and $b_{\boldsymbol{q}}$ are the creation and annihilation operators for molecules in the closed channel of our phenomenological model with $[b_{\boldsymbol{q}}, b^{\dagger}_{\boldsymbol{q}'}] = \delta_{\boldsymbol{q},\boldsymbol{q}'}$, and the summation $\sum'_{\boldsymbol{k},\boldsymbol{k}'}$ is done for $|\boldsymbol{k}-\boldsymbol{k}'|/2 < k_c$. The renormalization relation for cases without SOC is given in Ref. [41]. In the presence of Rashba SOC, The parameters $v(\boldsymbol{q})$ and $u(\boldsymbol{q})$ are now given by

$$\frac{1}{\kappa\left(E_b,\boldsymbol{q}\right)} = g(\boldsymbol{q}) + \frac{u(\boldsymbol{q})^2}{E_b - v(\boldsymbol{q})^2} \quad (55)$$

and

$$\frac{\left(\frac{u(\boldsymbol{q})}{E_b-v(\boldsymbol{q})}\right)^2}{\left(g(\boldsymbol{q})+\frac{u(\boldsymbol{q})^2}{E_b-v(\boldsymbol{q})}\right)^2} = \frac{\sum_{n_z=1}^{\infty}\left|\phi_{n_z}(0)\right|^2 \chi\left(E_b - n_z\omega,\boldsymbol{q}\right)}{\left|\phi_0(0)\right|^2}, \quad (56)$$

where the functions $\kappa(\eta,\boldsymbol{q})$ and $\chi(\eta,\boldsymbol{q})$ are defined as

$$\kappa(\eta,\boldsymbol{q}) = -2\pi\ln k_c + \pi\ln|\eta| + (2\pi)^2\lambda(\eta,\boldsymbol{q}) \quad (57)$$

and

$$\chi(\eta,\boldsymbol{q}) = \sum_{\boldsymbol{\alpha}}\int_{k<k_c} d\boldsymbol{k}\frac{\left|\langle 0,0|\boldsymbol{\alpha}(\boldsymbol{q},\boldsymbol{k})\rangle\right|^2}{\left(\eta-\varepsilon_c\right)^2}, \quad (58)$$

with $c = (\boldsymbol{\alpha},\boldsymbol{q},\boldsymbol{k})$. In Appendix F, we show that the 2D bound state $|\Psi_b^{(\text{eff})}(\boldsymbol{r})\rangle$ given by V_b has the same binding energy as the quasi-2D bound state $|\Psi_b(\boldsymbol{r})\rangle$ obtained in the previous section. Besides, it is also proven that the open-channel probability of $|\Psi_b^{(\text{eff})}(\boldsymbol{r})\rangle$ recovers the population of the transversal ground-state $|\Psi_b(\boldsymbol{r})\rangle$. Therefore, the effective 2D potential V_b can be used to study low-energy physics where nearly all particles are in the bound states with zero center-of-mass momentum.

V. CONCLUSIONS

In this paper we investigate the two-body physics of two-component fermonic atoms in 2D and quasi-2D configurations with a Rashba SOC. For the 2D case, we find that when the total momentum is zero, the logarithmic behavior of the 2D scattering amplitude in the low-energy limit is replaced by a polynomial behavior. For the quasi-2D system, we obtain an analytic expression of the effective 2D scattering amplitude as a function of the 3D scattering length a and the trapping frequency ω along the strongly confined z-direction, and observe the same polynomial behavior. We also discuss the two-atom bound state, and get the algebraic equation for the binding energy. We find that the two-body binding energy is enhanced by the presence of SOC, as a consequence of the increase of single particle density of states in the low energy limit. We also analyze the dispersion relation and extract the effective mass of the dimers. These information allows us to tune the effective 2D physics in quasi-2D configuration with parameters a and ω.

With the knowledge of two-body physics, we further construct two effective 2D Hamiltonians, which can individually mimic the original quasi-2D Hamiltonian within the energy regimes around the two-body binding energy or close to the single-particle threshold. These effective models can be used to analyze many-body physics of the system, hence help paving a way towards the simulation of 2D Fermi system with quasi-2D atomic gases. Our method developed in this paper can be directly generalized to systems of bosonic or distinguishable atoms with arbitrary type of SOC.

Acknowledgments

We thank Xiaoling Cui and Hui Zhai for helpful discussion. This work is supported by National Natural Science Foundation of China (11074305, 10904172), the NKBRSF of China (Grant No. 2012CB922104), the Fundamental Research Funds for the Central Universities, and the Research Funds of Renmin University of China (10XNL016). PZ and WZ would also like to thank the NCET Program for support.

Appendix A: wave functions of 2D scattering states and bound states

In this appendix we derive the Eqs. (10, 30) for 2D and quasi-2D low-energy scattering states, as well as Eqs. (21, 41) for 2D and quasi-2D bound states.

We first prove Eq. (10) for the 2D scattering wave function $|\psi_c^{(+)}(\boldsymbol{\rho})\rangle$. The Lippmann-Schwinger equation gives

$$|\psi_c^{(+)}(\boldsymbol{\rho})\rangle = |\psi_c^{(0)}(\boldsymbol{\rho})\rangle + \int d\boldsymbol{\rho}' g(\varepsilon_c;\boldsymbol{\rho},\boldsymbol{\rho}')V_{\rm 2D}(\boldsymbol{\rho}')\,|\psi_c^{(+)}(\boldsymbol{\rho}')\rangle. \tag{A1}$$

Here, $|\psi_c^{(0)}(\boldsymbol{\rho})\rangle$ is the incident state and the free Green's function $g(\varepsilon_c;\boldsymbol{\rho},\boldsymbol{\rho}')$ is defined in Eq. (12). Since the potential $V_{\rm 2D}(\boldsymbol{\rho})$ is negligible in the region $\rho \gtrsim \rho_*$, the integration in Eq. (A1) is only effective in the region $\rho' \lesssim \rho_*$. On the other hand, in the low-energy cases $k \ll 1/\rho_*$, when $\rho \to \infty$ and $\rho' \lesssim \rho_*$, the function $g(\varepsilon_c;\boldsymbol{\rho},\boldsymbol{\rho}')$ becomes very steady with respect to $\boldsymbol{\rho}'$ and we have

$$g(\varepsilon_c;\boldsymbol{\rho},\boldsymbol{\rho}') \approx g(\varepsilon_c;\boldsymbol{\rho},\mathbf{0}). \tag{A2}$$

Therefore, in the limit $\rho \to \infty$, the solution of Eq. (A1) takes the form

$$|\psi_c^{(+)}(\boldsymbol{\rho})\rangle = |\psi_c^{(0)}(\boldsymbol{\rho})\rangle + g(\varepsilon_c;\boldsymbol{\rho},\mathbf{0})|\chi\rangle, \tag{A3}$$

where the spin state $|\chi\rangle$ is related to $|\psi_c^{(+)}(\boldsymbol{\rho})\rangle$ via the equation

$$|\chi\rangle = \int d\boldsymbol{\rho}' V_{\rm 2D}(\boldsymbol{\rho}')\,|\psi_c^{(+)}(\boldsymbol{\rho}')\rangle. \tag{A4}$$

On the other hand, since $|\psi_c^{(+)}(\boldsymbol{\rho})\rangle$ is an eigen-state of $H_0^{(\rm 2D)}(\boldsymbol{q}) + V_{\rm 2D}(\boldsymbol{\rho})$ and the potential $V_{\rm 2D}(\boldsymbol{\rho})$ is negligible in the region $\rho \gtrsim \rho_*$, in such a region the wave function $|\psi_c^{(+)}(\boldsymbol{\rho})\rangle$ satisfies the equation

$$H_0^{(\rm 2D)}|\psi_c^{(+)}(\boldsymbol{\rho})\rangle = \varepsilon_c|\psi_c^{(+)}(\boldsymbol{\rho})\rangle. \tag{A5}$$

Therefore, the behavior of the wave function $|\psi_c^{(+)}(\boldsymbol{\rho})\rangle$ in the region $\rho \gtrsim \rho_*$ is determined by Eq. (A5) and the boundary condition (A3) in the limit $\rho \to \infty$. It is easy to prove that, the function $|\psi_c^{(0)}\rangle + g(\varepsilon_c;\boldsymbol{\rho},\mathbf{0})|\chi\rangle$ satisfies both of the two conditions. Therefore, $|\psi_c^{(+)}(\boldsymbol{\rho})\rangle$ satisfies Eq. (A5) not only in the limit $\rho \to \infty$, but also in the entire region of $\rho \gtrsim \rho_*$.

Furthermore, due to the facts $\hat{P}_{12}V_{\rm 2D}(\boldsymbol{\rho})\,\hat{P}_{12} = V_{\rm 2D}(\boldsymbol{\rho})$ and $\hat{P}_{12}|\psi_c^{(+)}(\boldsymbol{\rho})\rangle = -|\psi_c^{(+)}(\boldsymbol{\rho})\rangle$ with $\hat{P}_{12}$ the permutation operator of the two atoms, the integration (A4) can be re-written as

$$\begin{aligned}&\int d\boldsymbol{\rho}' V_{\rm 2D}(\boldsymbol{\rho}')\,|\psi_c^{(+)}(\boldsymbol{\rho}')\rangle \\ &= |0,0\rangle \int d\boldsymbol{\rho}' V_{\rm 2D}(\boldsymbol{\rho}')\,\langle 0,0|\psi_c^{(+)}(\boldsymbol{\rho}')\rangle.\end{aligned} \tag{A6}$$

Thus, $|\chi\rangle$ can be expressed as

$$|\chi\rangle = A(c)\,|0,0\rangle \tag{A7}$$

with $A(c)$ a c-number. Substituting Eq. (A7) into (A3), we finally obtain Eq. (10).

It is easy to find that Eqs. (30, 21) and (41) can be proved within the same approach. Especially, we have the result

$$\frac{A_{\rm eff}(c)}{\varphi_0(0)}|0,0\rangle = \int d\boldsymbol{r}' V_{\rm 3D}(r')\,|\Psi_c^{(+)}(\boldsymbol{r}')\rangle. \tag{A8}$$

which is similar as the ones in Eqs. (A4) and (A7).

Appendix B: small-distance behavior of 2D and quasi-2D wave function

In this appendix we prove Eqs. (13, 32, 22, 42) for the behaviors of the 2D and quasi-2D wave functions in the small-distance region $\rho_* << \rho << 1/k$ or $r_* << r << 1/k$. Here we only show the proof of Eqs. (13, 32). Eqs. (22, 42) can be derived with the same method.

We first prove Eq. (13) for the behavior of $|\psi_c^{(+)}(\boldsymbol{\rho})\rangle$. To this end, we define a rotated wave function

$$|\tilde{\psi}_c^{(+)}(\boldsymbol{\rho})\rangle = U(\boldsymbol{\rho})\,|\psi_c^{(+)}(\boldsymbol{\rho})\rangle \tag{B1}$$

with the unitary transformation $U(\boldsymbol{\rho})$ defined as

$$U(\boldsymbol{\rho}) = \exp\left[-\frac{i\xi x}{4}\left(\sigma_x^{(1)} - \sigma_x^{(2)}\right)\right]\exp\left[-\frac{i\xi y}{4}\left(\sigma_y^{(1)} - \sigma_y^{(2)}\right)\right]. \tag{B2}$$

Then the eigen-equation

$$H^{(\rm 2D)}|\psi_c^{(+)}(\boldsymbol{\rho})\rangle = \varepsilon_c|\psi_c^{(+)}(\boldsymbol{\rho})\rangle \tag{B3}$$

satisfied by $|\psi_c^{(+)}(\boldsymbol{\rho})\rangle$ gives

$$\tilde{H}^{(\rm 2D)}|\tilde{\psi}_c^{(+)}(\boldsymbol{\rho})\rangle = \varepsilon_c|\tilde{\psi}_c^{(+)}(\boldsymbol{\rho})\rangle, \tag{B4}$$

where

$$\begin{aligned}\tilde{H}^{(2\mathrm{D})} &= U(\boldsymbol{\rho})\, H^{(2\mathrm{D})} U^{\dagger}(\boldsymbol{\rho}) \\ &= -\sum_{\beta=x,y}\frac{\partial^2}{\partial\beta^2} - iW(\boldsymbol{\rho})\left(\frac{\partial}{\partial y}\right) + W'(\boldsymbol{q},\boldsymbol{\rho}) + \tilde{V}_{2\mathrm{D}}(\rho) \\ &\equiv \tilde{H}_0^{(2\mathrm{D})} + \tilde{V}_{2\mathrm{D}}(\rho)\end{aligned} \tag{B5}$$

Here, we have $\tilde{V}_{2\mathrm{D}} = UV_{2\mathrm{D}}U^{\dagger}$ and the operators $W(\boldsymbol{\rho})$ and $W'(\boldsymbol{q},\boldsymbol{\rho})$ are defined as

$$W(\boldsymbol{\rho}) = -\xi\left(\sigma_y^{(1)} - \sigma_y^{(2)}\right) + \xi U^{\dagger}\left(\sigma_y^{(1)} - \sigma_y^{(2)}\right)U \tag{B6}$$

and

$$\begin{aligned}W'(\boldsymbol{q},\boldsymbol{\rho}) &= -\frac{\xi^2}{16}\sum_{\alpha=x,y}U^{\dagger}(\boldsymbol{\rho})\left(\sigma_\alpha^{(1)} - \sigma_\alpha^{(2)}\right)^2 U(\boldsymbol{\rho}) \\ &\quad+\frac{\xi}{4}\sum_{\alpha=x,y}q_\alpha U^{\dagger}(\boldsymbol{\rho})\left(\sigma_\alpha^{(1)} - \sigma_\alpha^{(2)}\right)U(\boldsymbol{\rho}) \\ &\quad+\frac{W(\boldsymbol{\rho})^2}{16} - \frac{i}{2}\frac{\partial}{\partial y}W(\boldsymbol{\rho}).\end{aligned} \tag{B7}$$

Due to the weak SOC condition $\xi << 1/\rho_*$, in the region $\rho \ll 4/\xi$ we have we have $W(\boldsymbol{\rho}) \approx 0$ and $W'(\boldsymbol{q},\boldsymbol{\rho}) \approx W'(\boldsymbol{q},\boldsymbol{0})$. Therefore, in this region the rotated wave function $|\tilde{\psi}_c^{(+)}(\boldsymbol{\rho})\rangle$ is determined by the Hamiltonian

$$-\sum_{\beta=x,y}\frac{\partial^2}{\partial\beta^2} + W'(\boldsymbol{q},\boldsymbol{0}) + \tilde{V}_{2\mathrm{D}}(\rho) \tag{B8}$$

without SOC. Then the behavior of $|\tilde{\psi}_c^{(+)}(\boldsymbol{\rho})\rangle$ in the small-distance region is the same as the one for the 2D scattering wave function between two fermions without SOC, and can be described as

$$|\tilde{\psi}_c^{(+)}(\boldsymbol{\rho})\rangle \propto (\ln\rho - \ln d)\,|0,0\rangle. \tag{B9}$$

with the characteristic length d determined by the detail of $\tilde{V}_{2\mathrm{D}}(\boldsymbol{\rho})$. Using the relation $|\psi_c^{(+)}(\boldsymbol{\rho})\rangle = U^{\dagger}(\boldsymbol{\rho})\,|\tilde{\psi}_c^{(+)}(\boldsymbol{\rho})\rangle$, we immediately get the result in Eq. (13) for the small-distance behavior of $|\psi_c^{(+)}(\boldsymbol{\rho})\rangle$.

Eq. (32) can be proved with the similar approach. We can define the quasi-2D rotated wave function

$$|\tilde{\Psi}_c^{(+)}(\boldsymbol{r})\rangle = U(\boldsymbol{r})\,|\Psi_c^{(+)}(\boldsymbol{r})\rangle. \tag{B10}$$

Then $|\tilde{\Psi}_c^{(+)}(\boldsymbol{r})\rangle$ satisfies

$$\left[\tilde{H}_0^{(2\mathrm{D})} + H_z + \tilde{V}_{3\mathrm{D}}(\boldsymbol{r})\right]|\tilde{\Psi}_c^{(+)}(\boldsymbol{r})\rangle = \varepsilon_c|\tilde{\Psi}_c^{(+)}(\boldsymbol{r})\rangle, \tag{B11}$$

with $\tilde{H}_0^{(2\mathrm{D})}$ defined in Eq. (B5) and $\tilde{V}_{3\mathrm{D}} = UV_{3\mathrm{D}}U^{\dagger}$. Similar as above, in the region $r \ll 4/\xi$ we have $W(\boldsymbol{\rho}) \approx 0$ and $W'(\boldsymbol{q},\boldsymbol{\rho}) \approx W'(\boldsymbol{q},\boldsymbol{0})$, and $|\tilde{\Psi}_c^{(+)}(\boldsymbol{r})\rangle$ is determined by the Hamiltonian

$$-\sum_{\beta=x,y}\frac{\partial^2}{\partial\beta^2} + H_z + W'(\boldsymbol{q},\boldsymbol{0}) + \tilde{V}_{3\mathrm{D}}(\boldsymbol{r}) \tag{B12}$$

without SOC. Then the behavior of $|\tilde{\Psi}_c^{(+)}(\boldsymbol{r})\rangle$ in the small-distance region is the same as the one for the 3D scattering wave function between two fermions without SOC, and can be described as

$$|\tilde{\Psi}_c^{(+)}(\boldsymbol{r})\rangle \propto \left(\frac{1}{r} - \frac{1}{a}\right)|0,0\rangle, \tag{B13}$$

with the scattering length a determined by the detail of $\tilde{V}_{3\mathrm{D}}(\boldsymbol{r})$. Using the relation $|\Psi_c^{(+)}(\boldsymbol{r})\rangle = U^{\dagger}(\boldsymbol{r})\,|\tilde{\Psi}_c^{(+)}(\boldsymbol{r})\rangle$, we obtain the behavior of $|\Psi_c^{(+)}(\boldsymbol{r})\rangle$ in the small-distance region:

$$|\Psi_c^{(+)}(\boldsymbol{r})\rangle \propto \left(\frac{1}{r} - \frac{1}{a}\right)|0,0\rangle + \frac{i\xi}{4}\sum_{\beta=x,y}\frac{\beta}{r}\left(\sigma_\beta^{(1)} - \sigma_\beta^{(2)}\right)|0,0\rangle. \tag{B14}$$

Then we have the result in Eq. (32):

$$\langle 0,0|\Psi_c^{(+)}(\boldsymbol{r})\rangle \propto \left(\frac{1}{r} - \frac{1}{a}\right). \tag{B15}$$

In the end of this appendix, we point out that, the results in Eqs. (B9) and (B13) of this appendix can be proved more explicitly with the approach given in Ref. [43].

Appendix C: small-distance behavior of 2D and quasi-2D Green's function

In this appendix we prove Eqs. (14, 33) for the behavior of the functions $\langle 0,0|g(\varepsilon_c;\boldsymbol{\rho},\boldsymbol{0})|0,0\rangle$ and $\langle 0,0|G(\varepsilon_c;\boldsymbol{r},\boldsymbol{0})|0,0\rangle$ in the small-distance region. We begin from Eq. (14). In the small-distance region $\rho_* \lesssim \rho << 1/k$, the function $\langle 0,0|g(\varepsilon_c;\boldsymbol{\rho},\boldsymbol{0})|0,0\rangle$ is governed by the leading terms in the limit $\rho \to 0$. Using the facts

$$\delta(\boldsymbol{\rho} - \boldsymbol{\rho}') = \int d\boldsymbol{k}\frac{e^{i\boldsymbol{k}\cdot(\boldsymbol{\rho}-\boldsymbol{\rho}')}}{(2\pi)^2}\left(\sum_{\boldsymbol{\alpha}}|\boldsymbol{\alpha}(\boldsymbol{q},\boldsymbol{k})\rangle\langle\boldsymbol{\alpha}(\boldsymbol{q},\boldsymbol{k})|\right) \tag{C1}$$

and

$$H_0^{(2\mathrm{D})}\left(e^{i\boldsymbol{k}\cdot\boldsymbol{\rho}}|\boldsymbol{\alpha}(\boldsymbol{q},\boldsymbol{k})\rangle\right) = \varepsilon_c\left(e^{i\boldsymbol{k}\cdot\boldsymbol{\rho}}|\boldsymbol{\alpha}(\boldsymbol{q},\boldsymbol{k})\rangle\right), \tag{C2}$$

it is easy to show that

$$\begin{aligned}&\langle 0,0|g(\varepsilon_c;\boldsymbol{\rho},\boldsymbol{0})|0,0\rangle \\ &= \sum_{\boldsymbol{\alpha}'}\int d\boldsymbol{k}'\frac{e^{i\boldsymbol{k}'\cdot\boldsymbol{\rho}}}{(2\pi)^2}\frac{\left|\langle 0,0|\boldsymbol{\alpha}'(\boldsymbol{q},\boldsymbol{k}')\rangle\right|^2}{\varepsilon_c + i0^+ - \varepsilon_{c'}} \\ &= \int d\boldsymbol{k}'\frac{e^{i\boldsymbol{k}'\cdot\boldsymbol{\rho}}}{(2\pi)^2}\frac{1}{\varepsilon_c + i0^+ - |\boldsymbol{k}'|^2} \\ &\quad+\sum_{\boldsymbol{\alpha}}\int d\boldsymbol{k}'\frac{e^{i\boldsymbol{k}'\cdot\boldsymbol{\rho}}}{(2\pi)^2}\left|\langle 0,0|\boldsymbol{\alpha}(\boldsymbol{q},\boldsymbol{k}')\rangle\right|^2 \times \\ &\quad\left(\frac{1}{\varepsilon_c + i0^+ - \varepsilon_{c'}} - \frac{1}{\varepsilon_c + i0^+ - |\boldsymbol{k}'|^2}\right).\end{aligned} \tag{C3}$$

with $c' = (\boldsymbol{\alpha}'; \boldsymbol{q}; \boldsymbol{k}')$. Using the fact

$$\int d\boldsymbol{k}' \frac{e^{i\boldsymbol{k}'\cdot\boldsymbol{\rho}}}{(2\pi)^2} \frac{1}{\varepsilon_c + i0^+ - |\boldsymbol{k}'|^2} = -\frac{K_0\left(-i\sqrt{\varepsilon_c}\rho\right)}{2\pi} \tag{C4}$$

with K_0 the modified Bessel function, we get the result

$$\begin{aligned} & \langle 0,0|g(\varepsilon_c;\boldsymbol{\rho},\boldsymbol{0})|0,0\rangle \\ = & -\frac{1}{2\pi}K_0\left(-i\sqrt{\varepsilon_c}\rho\right) \\ & +\sum_{\boldsymbol{\alpha}}\int d\boldsymbol{k}'\frac{e^{i\boldsymbol{k}'\cdot\boldsymbol{\rho}}}{(2\pi)^2}\left|\langle 0,0|\boldsymbol{\alpha}\left(\boldsymbol{q},\boldsymbol{k}'\right)\rangle\right|^2\times \\ & \left(\frac{1}{\varepsilon_c+i0^+-\varepsilon_{c'}}-\frac{1}{\varepsilon_c+i0^+-|\boldsymbol{k}'|^2}\right). \end{aligned} \tag{C5}$$

In the small-distance region we have

$$-\frac{1}{2\pi}K_0\left(-i\sqrt{\varepsilon_c}\rho\right) \approx \frac{\ln\rho + C + \ln\left(-\frac{i\sqrt{\varepsilon_c}}{2}\right)}{2\pi} \tag{C6}$$

and

$$\begin{aligned} & \sum_{\boldsymbol{\alpha}}\int d\boldsymbol{k}'\frac{e^{i\boldsymbol{k}'\cdot\boldsymbol{\rho}}}{(2\pi)^2}\left|\langle 0,0|\boldsymbol{\alpha}\left(\boldsymbol{q},\boldsymbol{k}'\right)\rangle\right|^2\times \\ & \left(\frac{1}{\varepsilon_c+i0^+-\varepsilon_{c'}}-\frac{1}{\varepsilon_c+i0^+-|\boldsymbol{k}'|^2}\right) \\ \approx & \ \lambda(\varepsilon_c,\boldsymbol{q}). \end{aligned} \tag{C7}$$

with λ-function defined in Eq. (15). Then we have proved Eq. (14).

Eq. (33) can be proved with the similar approach. In the small-distance region $r_* \lesssim r << 1/k$, the function $\langle 0,0|G(\varepsilon_c;\boldsymbol{\rho},\boldsymbol{0})|0,0\rangle$ is governed by the leading terms in the limit $r\to 0$. Using the facts

$$\begin{aligned} \delta\left(\boldsymbol{r}-\boldsymbol{r}'\right) = & \int d\boldsymbol{k}\frac{e^{i\boldsymbol{k}\cdot(\boldsymbol{\rho}-\boldsymbol{\rho}')}}{(2\pi)^2}\left(\sum_{\boldsymbol{\alpha}}|\boldsymbol{\alpha}\left(\boldsymbol{q},\boldsymbol{k}\right)\rangle\langle\boldsymbol{\alpha}\left(\boldsymbol{q},\boldsymbol{k}\right)|\right) \\ & \times\left(\sum_n\varphi_{n_z}\left(z\right)\varphi_{n_z}\left(z'\right)\right) \end{aligned} \tag{C8}$$

and

$$\begin{aligned} & \left(H_0^{(2\mathrm{D})}+H_z\right)\varphi_{n_z}\left(z\right)e^{i\boldsymbol{k}\cdot\boldsymbol{\rho}}|\boldsymbol{\alpha}\left(\boldsymbol{q},\boldsymbol{k}\right)\rangle \\ = & \left(n\omega+\varepsilon_c\right)\varphi_{n_z}\left(z\right)e^{i\boldsymbol{k}\cdot\boldsymbol{\rho}}|\boldsymbol{\alpha}\left(\boldsymbol{q},\boldsymbol{k}\right)\rangle, \end{aligned} \tag{C9}$$

it is easy to prove that

$$\begin{aligned} & \lim_{r\to 0}\langle 0,0|G(\varepsilon_c;\boldsymbol{r},\boldsymbol{0})|0,0\rangle \\ = & \lim_{r\to 0}\frac{1}{\varepsilon_c+i0^+-\left[-\sum_{\alpha=x,y}\frac{\partial^2}{\partial\alpha^2}+H_z\right]}\delta\left(\boldsymbol{r}\right) \\ & +\sum_{n_z=0}^{\infty}|\varphi_{n_z}(0)|^2\lambda(\varepsilon_c-n_z\omega;\boldsymbol{q}) \end{aligned} \tag{C10}$$

As shown in Ref. [38], we have

$$\begin{aligned} & \lim_{r\to 0}\frac{1}{\varepsilon_c+i0^+-\left[-\sum_{\alpha=x,y}\frac{\partial^2}{\partial\alpha^2}+H_z\right]}\delta\left(\boldsymbol{r}\right) \\ = & -\frac{1}{4\pi}\frac{1}{r}-\frac{w\left(\varepsilon_c/2\right)}{2\left(2\pi\right)^{3/2}l_0} \end{aligned} \tag{C11}$$

with the function $w\left(\eta\right)$ defined in Eq. (34). Substituting Eqs (C11) into Eq. (C10), we can get Eq. (33).

Appendix D: Scattering amplitudes in 2D and quasi-2D geometries with SOC

In this appendix we proof Eqs. (20) and (39) for the 2D and quasi-2D scattering amplitude. The 2D scattering amplitude $f^{(2\mathrm{D})}\left(c'\leftarrow c\right)$ between the incident state $|\psi_c^{(0)}\left(\boldsymbol{\rho}\right)\rangle$ and out-put state $|\psi_{c'}^{(+)}\left(\boldsymbol{\rho}\right)\rangle$ is defined as

$$f^{(2\mathrm{D})}\left(c'\leftarrow c\right) = -2\pi^2\int d\boldsymbol{\rho}\langle\psi_{c'}^{(0)}\left(\boldsymbol{\rho}\right)|\ V_{2\mathrm{D}}(\rho)\,|\psi_c^{(+)}\left(\boldsymbol{\rho}\right)\rangle, \tag{D1}$$

In the region $\rho' \lesssim \rho_*$ we have

$$\langle\psi_{c'}^{(0)}\left(\boldsymbol{\rho}\right)| \approx \langle\psi_{c'}^{(0)}\left(\boldsymbol{0}\right)|. \tag{D2}$$

Substituting Eq. (D2) into (D1), we immediately obtain the result in Eq. (20):

$$f^{(2\mathrm{D})}\left(c'\leftarrow c\right) = -2\pi^2\langle\psi_{c'}^{(0)}\left(\boldsymbol{0}\right)|0,0\rangle A\left(c\right). \tag{D3}$$

Eq. (39) for the quasi-2D scattering amplitude $f^{(\mathrm{Q2D})}$ can be proved in the same approach. The definition of $f^{(\mathrm{Q2D})}$ is

$$f^{(2\mathrm{D})}\left(c'\leftarrow c\right) = -2\pi^2\int d\boldsymbol{r}\langle\Psi_{c'}^{(0)}\left(\boldsymbol{r}\right)|\ V_{3\mathrm{D}}(r)\,|\Psi_c^{(+)}\left(\boldsymbol{r}\right)\rangle. \tag{D4}$$

Using Eqs. (A8) and (29), we immediately get Eq. (39).

Appendix E: 2D scattering amplitude without SOC

In this appendix we derive the 2D scattering amplitude of two distinguishable atoms in systems without SOC [38]. In this case we have the incident wave function

$$\psi_{\boldsymbol{k}}^{(0)}\left(\boldsymbol{\rho}\right) = \frac{1}{2\pi}e^{i\boldsymbol{k}\cdot\boldsymbol{\rho}} \tag{E1}$$

with scattering energy $\varepsilon = k^2$. As shown in Appendix A and Ref. [38], the scattered wave function $\psi_{\boldsymbol{k}}^{(+)}\left(\boldsymbol{\rho}\right)$ and the 2D scattering amplitude $f^{(2\mathrm{D})}\left(\varepsilon\right)$ are given by

$$\psi_{\boldsymbol{k}}^{(+)}\left(\boldsymbol{\rho}\right) = \psi_{\boldsymbol{k}}^{(0)}\left(\boldsymbol{\rho}\right) + Ag_R(\varepsilon;\boldsymbol{\rho},\boldsymbol{0}); (\rho \gtrsim \rho_*) \tag{E2}$$

and

$$f^{(2\mathrm{D})}\left(\varepsilon\right) = -\pi A. \tag{E3}$$

Here, we have

$$g_R(\varepsilon;\boldsymbol{\rho},\boldsymbol{\rho}') = {}_\perp\langle\boldsymbol{\rho}|\frac{1}{\varepsilon + i0^+ + \sum_{\alpha=x,y}\frac{\partial^2}{\partial\alpha^2}}\delta\left(\boldsymbol{\rho}-\boldsymbol{\rho}'\right) = -\frac{1}{2\pi}K_0\left(-i\sqrt{\varepsilon}\rho\right), \tag{E4}$$

where K_0 is the modified Bessel function of the second type. The coefficient A can be determined by considering that $\psi(\boldsymbol{\rho}) \propto \ln\rho - \ln d$ in the region $\rho_* \lesssim \rho \ll 1/\sqrt{\varepsilon}$, with d the characteristic length. Using this condition and the expression (E4) of $g_R(\varepsilon;\boldsymbol{\rho},\mathbf{0})$, we get the coefficient A and then the 2D scattering amplitude $f_0^{(2\mathrm{D})}$:

$$f_0^{(2\mathrm{D})}(\varepsilon) = \frac{\pi\psi_{\boldsymbol{k}}^{(0)}(\mathbf{0})}{i\frac{1}{4} - \frac{1}{2\pi}\left(\ln d + C + \ln\frac{\sqrt{\varepsilon}}{2}\right)}, \tag{E5}$$

where $C = 0.5772...$ is the Euler gamma number.

The expression (E5) clearly describes the character of the 2D low-energy scattering. It shows that the low-energy scattering amplitude $f_0^{(2\mathrm{D})}(\varepsilon)$ is totally determined by the parameter d. In particular, $f_0^{(2\mathrm{D})}(\varepsilon)$ logarithmically decays to zero [38] in the limit $\varepsilon \to 0$, and achieves the maximum when $\varepsilon = 4\exp(-2C)/d^2$.

Appendix F: Renormalization of the effective 2D interaction

In this appendix we prove Eqs. (53, 55) and (56) for the renormalization of the effective 2D interaction potentials $\hat{V}_o$ and $\hat{V}_b$. For the convenience of our calculation, in this appendix we do not work in the $\boldsymbol{\rho}$-representation as before. We use the Dirac vector $|\rangle_\perp$ to describe the quantum state of the 2D spatial relative motion of the two atoms, and $|\rangle_T$ for the total quantum state for both the relative motion and spin of the two atoms. Namely, the total quantum $|\psi\rangle_T$ and the spinor wave function $|\psi(\boldsymbol{\rho})\rangle$ defined in Eq. (1) is related as

$$|\psi\rangle_T = \int d\boldsymbol{\rho}|\psi(\boldsymbol{\rho})\rangle|\boldsymbol{\rho}\rangle_\perp, \tag{F1}$$

where $|\boldsymbol{\rho}\rangle_\perp$ is the eigen-state of the atomic relative coordinate.

We first consider the single-channel potential $\hat{V}_o$ defined in Eq. (52). To obtain the correct expression for the parameter g, we should calculate the 2D scattering amplitude given by $\hat{V}_o$. This scattering amplitude can be obtained from the Lippmman-Schwinger equation for the 2-body T-operator $\hat{T}_o$ with respect to $\hat{V}_o$:

$$\hat{T}_o(E) = \hat{V}_o + \hat{V}_o\hat{g}(E)\hat{V}_o(E), \tag{F2}$$

where the Green's operator $\hat{g}(\eta)$ is defined as

$$\hat{g}(\eta) = \frac{1}{\eta + i0^+ - H_0^{(2\mathrm{D})}}. \tag{F3}$$

and satisfies $g(\eta,\boldsymbol{\rho},\boldsymbol{\rho}') = {}_\perp\langle\boldsymbol{\rho}|\hat{g}(\eta)|\boldsymbol{\rho}'\rangle_\perp$ with $g(\eta,\boldsymbol{\rho},\boldsymbol{\rho}')$ defined in Eq. (12). Eq. (F2) can be solved directly with the first-quantization form of $\hat{V}_o$. We find that the on-shell element of $\hat{T}_o(E)$ has a separable expression

$$_T\langle\psi_{c'}^{(0)}|\hat{T}_o(\varepsilon_c)|\psi_c^{(0)}\rangle_T = \mathcal{V}(c')\,\mathcal{U}(c), \tag{F4}$$

where $|\psi_c^{(0)}\rangle_T$ is defined in Eq. (6) and we have $\varepsilon_c = \varepsilon_{c'}$. The functions $\mathcal{V}(c')$ and $\mathcal{U}(c)$ can be obtained from Eq. (F2). The 2D scattering amplitude given by V_o is

$$f_o(c' \leftarrow c) = -2\pi^2\ {}_T\langle\psi_{c'}^{(0)}|\hat{T}_o(\varepsilon_c)|\psi_c^{(0)}\rangle_T. \tag{F5}$$

As shown in Sec. IV, the 2D scattering amplitude given by V_o should be the same as the quasi-2D scattering amplitude, and then we should have

$$f_o(c' \leftarrow c) = f^{(\mathrm{Q2D})}(c' \leftarrow c) \tag{F6}$$

with $f^{(\mathrm{Q2D})}$ defined in Eq. (39). This requirement directly leads to Eq. (53).

Now we consider the two-channel model $\hat{V}_b$ and prove the renormalization relations (55) and (56) of $\hat{V}_b$. To this end, we should calculate the bound state $|\Psi_b^{(\mathrm{eff})}\rangle_T$, which satisfies

$$|\Psi_b^{(\mathrm{eff})}\rangle_T = \hat{g}(E_b)\hat{V}_b|\Psi_b^{(\mathrm{eff})}\rangle_T. \tag{F7}$$

Equation (F7) can also be solved directly via the first-quantization form of $\hat{V}_b$. We can derive the energy E_b as well as the components of $|\Psi_b^{(\mathrm{eff})}\rangle_T$ in both the open and the close channels. As shown in Sec. IV, the energy E_b of $|\Psi_b^{(\mathrm{eff})}\rangle_T$ should be the same as that of the quasi-2D bound state $|\hat{\Psi}_b\rangle_T$, and then satisfies Eq. (43). The open-channel probability of $|\Psi_b^{(\mathrm{eff})}\rangle_T$ is the same as the transverse-ground-state probability of $|\Psi_b\rangle_T$, which is given in Eq. (41). These requirements directly lead to Eqs. (55) and (56).

---

[1] Y. -J. Lin, R. L. Compton, A. R. Perry, W. D. Phillips, J. V. Porto, and I. B. Spielman, Phys. Rev. Lett. **102**, 130401 (2009).

[2] Y.-J. Lin, K. Jiménez-García, and I. B. Spielman, Nature **471**, 83 (2011).

[3] H. Zhai, Int. J. Mod. Phys. B **26**, 1230001 (2012).

[4] Y.-J. Lin, R. L. Compton, K. Jiménez-García, J. V. Porto, and I. B. Spielman, Nature **462**, 628 (2009).

[5] Y.-J. Lin, R. L. Compton, K. Jiménez-García, W. D. Phillips, J. V. Porto, and I. B. Spielman, Nature Physics **7**, 531 (2011).

[6] J. Y. Zhang, S. C. Ji, Z. Chen, L. Zhang, Z. D. Du, B.

Yan, G. S. Pan, B. Zhao, Y. Deng, H. Zhai, S. Chen and J. W. Pan, Phys. Rev. Lett. **109**, 115301.

[7] Z. Fu, P. Wang, S. Chai, L. Huang, and J. Zhang, Phys. Rev. A 84, 043609 (2011).

[8] L. Zhang, J.-Y. Zhang, S.-C. Ji, Z.-D. Du, H. Zhai, Y. Deng, S. Chen, P. Zhang and J.-W. Pan, arXiv: 1208.4941.

[9] R. A. Williams, L. J. LeBlanc, K. Jiménez-García, M. C. Beeler, A. R. Perry, W. D. Phillips, and I. B. Spielman, Science **335**, 314 (2012).

[10] P. Wang, Z.-Q. Yu, Z. Fu, J. Miao, L. Huang, S. Chai, H. Zhai, and J. Zhang, Phys. Rev. Lett. **109**, 095301 (2012).

[11] L. W. Cheuk, A. T. Sommer, Z. Hadzibabic, T. Yefsah, W. S. Bakr, and M. W. Zwierlein, Phys. Rev. Lett. **109**, 095302 (2012).

[12] C.-J. Wu, I. M. Shem, and X.-F. Zhou, Chin. Phys. Lett. **28**, 097102 (2011).

[13] C. Wang, C. Gao, C.-M. Jian, and H. Zhai, Phys. Rev. Lett. **105**, 160403 (2010).

[14] T.-L. Ho and S. Zhang, Phys. Rev. Lett. **107**, 150403 (2011).

[15] Z. F. Xu, R. Lu, and L. You, Phys. Rev. A **83**, 053602 (2011).

[16] X.-Q. Xu and J. H. Han, Phys. Rev. Lett. **107**, 200401 (2011).

[17] X.-F Zhou, J. Zhou, and C. Wu, Phys. Rev. A **84**, 063624 (2011).

[18] S. Sinha, R. Nath, and L. Santos, Phys. Rev. Lett. **107**, 270401 (2011).

[19] H. Hu, B. Ramachandhran, H. Pu, and X.-J. Liu, Phys. Rev. Lett. **108**, 010402 (2012); B. Ramachandhran, B. Opanchuk, X.-J. Liu, H. Pu, P. D. Drummond, and H. Hu, Phys. Rev. A **85**, 023606 (2012).

[20] X. Cui, Phys. Rev. A 85, 022705 (2012).

[21] J. P. Vyasanakere and V. B. Shenoy, Phys. Rev. B **83**, 094515 (2011); J. P. Vyasanakere, S. Zhang, and V. B. Shenoy, Phys. Rev. B **84**, 014512 (2011).

[22] M. Gong, S. Tewari, and C. Zhang, Phys. Rev. Lett. **107**, 195303 (2011).

[23] Z.-Q. Yu and H. Zhai, Phys. Rev. Lett. **107**, 195305 (2011).

[24] H. Hu, L. Jiang, X.-J. Liu, and H. Pu, Phys. Rev. Lett. **107**, 195304 (2011).

[25] M. Iskin and A. L. Subasi, Phys. Rev. Lett. **107**, 050402 (2011).

[26] W. Yi and G.-C. Guo, Phys. Rev. A **84**, 031608(R) (2011).

[27] L. Han and C. A. R. Sa de Melo, Phys. Rev. A **85**, 011606(R) (2012).

[28] L. Dell'Anna, G. Mazzarella, and L. Salasnich, Phys. Rev. A **84**, 033633 (2011).

[29] J. Zhou, W. Zhang, and W. Yi, Phys. Rev. A **84**, 063603 (2011).

[30] G. Chen, M. Gong, and C. Zhang, Phys. Rev. A **85**, 013601 (2012).

[31] K. Seo, L. Han, and C. A. R. Sa de Melo, Phys. Rev. A **85**, 033601 (2012).

[32] B. Huang and S. Wan, arXiv:1109.3970.

[33] L. He and X.-G. Huang, Phys. Rev. Lett. **108**, 145302 (2012).

[34] S. Takei, C.-H Lin, B. M. Anderson, and V. Galitski, Phys. Rev. A **85**, 023626 (2012).

[35] W. Yi and W. Zhang, arXiv: 1204.6476.

[36] M. Olshanii, Phys. Rev. Lett. **81**, 938 (1998).

[37] J. P. Kestner and L.-M. Duan, Phys. Rev. A **76**, 063610 (2007).

[38] D. S. Petrov and G. V. Shlyapnikov, Phys. Rev. A **64**, 012706 (2001).

[39] W. Zhang, G.-D. Lin, and L.-M. Duan, Phys. Rev. A **77**, 063613 (2008); Phys. Rev. A **78**, 043617 (2008).

[40] ....

[41] J. P. Kestner and L.-M. Duan, Phys. Rev. A **74**, 053606 (2006).

[42] J. R. Taylor, *Scattering Theory*, Wiley, New York, 1972.

[43] P. Zhang, L. Zhang, Y. Deng, arXiv:1208.5976.